Title

Antitumor effects of 4-Methylumbelliferone, a hyaluronan synthesis inhibitor, on malignant peripheral nerve sheath tumor

Kunihiro Ikuta[1], Takehiro Ota[1], Lisheng Zhuo[2], Hiroshi Urakawa[1], Eiji Kozawa[1], Shunsuke Hamada[1], Koji Kimata[2], Naoki Ishiguro[1], Yoshihiro Nishida[1]

[1]Department of Orthopaedic Surgery, Nagoya University Graduate School and School of Medicine
65 Tsurumai, Showa, Nagoya, 466-8550, Japan

[2]Research Complex for the Medicine Frontiers, Aichi Medical University, Yazako, Nagakute, Aichi, 480-1195, Japan

Corresponding and reprints request to Y. Nishida, Department of Orthopaedic Surgery, Nagoya University Graduate School and School of Medicine, 65 Tsurumai, Showa, Nagoya, 466-8550, Japan
Phone: 81-52-741-2111
Fax: 81-52-744-2260
E-mail: ynishida@med.nagoya-u.ac.jp

Key words; hyaluronan, 4-methylumbeliferone, malignant peripheral nerve sheath tumor, neurofibromatosis type 1

Article Category; Research Articles and Short Reports (Molecular Cancer Biology)

Novelty and Impact; A novel therapeutic tool other than existing chemotherapeutic agents is required to improve the prognosis of patients with malignant peripheral nerve sheath tumors (MPNSTs). This study demonstrates for the first time that 4-Methylumbelliferone (MU), an HA synthesis inhibitor, significantly suppress the tumorigenicity on human MPNST *in vitro* and *in vivo*. Our results suggest that MU may be a promising agent with novel antitumor mechanisms for MPNSTs.

Abstract

Hyaluronan (HA) has been shown to play important roles in the growth, invasion, and metastasis of malignant tumors. Our previous study showing that high HA expression in malignant peripheral nerve sheath tumors (MPNST) is predictive of poor patient prognosis, prompted us to speculate that inhibition of HA synthesis in MPNST might suppress the tumorigenicity. The aim of this study was to investigate the antitumor effects of 4-Methylumbelliferone (MU), an HA synthesis inhibitor, on human MPNST cells and tissues. The effects of MU on HA accumulation and tumorigenicity in MPNST cells were analyzed in the presence or absence of MU in an *in vitro* as well as *in vivo* xenograft model using human MPNST cell lines, sNF96.2 (primary recurrent) and sNF02.2 (metastatic). MU significantly inhibited cell proliferation, migration, and invasion in both MPNST cell lines. HA binding protein (HABP) staining, particle exclusion assay, and quantification of HA revealed that MU significantly decreased HA accumulation in the cytoplasms and pericellular matrices in both MPNST cell lines. The expression levels of HA synthase2 (HAS2) and HA synthase3 (HAS3) mRNA were downregulated after treatment with MU. MU induced apoptosis of sNF96.2 cells, but not sNF02.2 cells. MU administration significantly inhibited the tumor growth of sNF96.2 cells in the mouse xenograft model. To the best of our knowledge, this study demonstrates for the first time the antitumor effects of MU on human MPNST mediated by inhibition of HA synthesis. Our results suggest that MU may be a promising agent with novel antitumor mechanisms for MPNST.

Introduction

Malignant peripheral nerve sheath tumor (MPNST) is a rare soft tissue sarcoma with an aggressive clinical course and high metastatic potential even after adequate surgical resection. Half of the patients with MPNST have associated neurofibromatosis type 1 (NF1), a tumor suppressor gene syndrome with an incidence of 1 in 3,500, whereas the remainder develop these tumors *de novo*.[1] Approximately 10% of patients with NF1 develop MPNST which is the leading cause of NF1-related mortality.[2] Currently, optimal surgery remains the cornerstone of treatment for localized MPNST, whereas there is no effective systemic therapy available for advanced or metastatic MPNST. The prognosis for patients with MPNST is generally unfavorable with a 5-year survival rate of 20–50%.[3] The development of novel antitumor agents is urgently needed to improve the survival of patients with MPNST.

Hyaluronan (HA) is a high-molecular-weight glycosaminoglycan that is one of the major components of the extracellular matrix (ECM). HA is synthesized by three types of HA synthases (HAS1, HAS2, and HAS3) at the intracellular border of the plasma membrane and is extruded to the cell surface and extracellular matrices.[4] It is known that HA plays important roles in matrix assembly, cell proliferation, differentiation, and migration during development, normal tissue homeostasis, and disease.[5] Moreover, previous studies have described that extracellular HA stimulates growth, migration, and invasion of various malignant tumors,[6,7] and that increased HA levels in tumor tissues are correlated with a poor patient prognosis with malignancies such as ovarian, lung, thyroid, breast, colorectal, and gastric cancers.[8–13] Furthermore, antisense inhibition of HAS genes in tumor cells inhibits proliferation, invasion, and motility *in vitro* and tumor growth and metastasis in *in vivo* models.[14–17]

4-Methylumbelliferone (MU), a coumarin derivative (7-hydroxy-4-methylcoumarin),

blocks HA synthesis by inhibiting glucuronidation by endogenous glucuronosyltransferase, which results in depletion of uridine diphosphate glucuronic acid.[18] To date, several studies have investigated the antitumor effects of MU in cancer cell lines and in *in vivo* models.[19–22] Recently, it was described that MU exerts potent antitumor effects against bone metastases of breast and lung cancers.[23,24] However, no studies have ever analyzed the inhibitory effects of MU on soft tissue sarcoma, particularly on malignant sheath tumors. The consensus from these studies was that MU inhibits the tumorigenicity of multiple tumor cell types through inhibition of HA synthesis both *in vitro* and *in vivo*. It was also shown that MU possibly downregulates expression levels of HAS2 and/or HAS3 mRNA in several cancer cell lines.[20,21,23] Based on these findings, MU is thought to inhibit HA production of tumor cells in at least two ways, namely inhibition of glucuronidation and HASs expression.[20,25]

We previously demonstrated that increased HA expression in tumor tissues could be a useful marker in differentiating MPNST from neurofibroma, and in identifying patients with MPNST having a poor prognosis.[26] Based on these findings, we hypothesized that HA-targeting therapy for patients with MPNST might have potential as a novel therapeutic tool. In this study, we examined the antitumor effects of MU on human MPNST cell lines *in vitro* and in an *in vivo* mouse xenograft model.

Materials and methods

Cell culture

The human MPNST cell lines, sNF96.2 and sNF02.2, were obtained from the American Type Culture Collection (Manassas, VA). sNF96.2 cells were derived from recurrent localized tumor and sNF02.2 from lung metastatic tumor of MPNST in NF1 patients, respectively. These two MPNST cell lines, which have different background (locally recurrent and metastatic tumors), were selected because antitumor effects of

MU should be evaluated with MPNST cells of various oncological behaviors. Doubling time (26h) of sNF02.2 was shorter than that (33h) of sNF96.2. The cells were cultured in Dulbecco's modified Eagle's medium (DMEM) supplemented with 10% fetal bovine serum (FBS), 100 U/ml penicillin, and 100 μg/ml streptomycin. The cells were maintained at 37°C in a humidified atmosphere with 5% CO_2. MU was purchased from Wako Pure Chemicals (Osaka, Japan). MU for *in vitro* experiments was dissolved in dimethylsulfoxide (DMSO; Sigma-Aldrich, St Louis, MO) as a stock solution, and the final concentration of DMSO in the medium was adjusted to 0.1%. To exclude the cytotoxicity of DMSO in each experiment, the cells in the control group were incubated with the same concentration of DMSO without MU. For analyses of *in vitro* experiments, both cell lines (sNF02.2 and sNF96.2) were used, whereas only sNF96.2 cells used for *in vivo* studies as hereinafter described.

HA staining for cells and tissues

HA accumulation in sNF96.2 and sNF02.2 cells and implanted tumors of sNF96.2 cells in the *in vivo* model was evaluated using biotinylated hyaluronic acid binding protein (b-HABP; Seikagaku, Tokyo, Japan) as previously described.[27,28] *In vitro*, sNF96.2 and sNF02.2 cells were seeded in chamber slides and allowed to adhere to the bottom of the slides overnight. The cells were incubated with (1.0 mM) or without MU (0.1% DMSO) for 24 h. The cultured cells were fixed with 4% paraformaldehyde buffered with phosphate buffered saline (PBS) at room temperature for 20 min. The slides were treated with 3% H_2O_2 in methanol for 10 min at room temperature to block the endogenous peroxidase activity, followed by incubation with 1 % bovine serum albumin (BSA) in PBS for 1 h at room temperature. The slides were then incubated with 2.0 μg/ml b-HABP probe for 2 h at room temperature. Bound b-HABP was detected by the addition of streptavidin-peroxidase reagents and diaminobenzidine-

containing substrate solution (Nichirei, Tokyo, Japan). The slides were counterstained with hematoxylin. The slides incubated without b-HABP were used as negative controls.

For tissue staining, *in vivo* specimens of sNF96.2 tumors were fixed overnight with 4% paraformaldehyde buffered with PBS, and then embedded in paraffin. Sections of 5-μm thickness were deparaffinized in xylene, rehydrated through graded ethanol, and subjected to HA staining as described above. Stained sections incubated without b-HABP or pre-treated with 5 U/ml Streptomyces hyaluronidase for 1 h at 60ºC were used as negative controls or to confirm the specificity of HABP staining.

Particle exclusion assay

Pericellular matrices were visualized using a particle exclusion assay.[29] Following the treatment of sNF96.2 and sNF02.2 cells for 48 h with (1.0 mM) or without MU (0.1% DMSO), the medium was replaced with a suspension of sheep erythrocytes (Sigma-Aldrich, St Louis, MO) in PBS. Visualized pericellular matrices were photographed with an inverted phase-contrast microscope. Ten cells were randomly selected at 10 different fields in each treatment, and the functional pericellular matrix areas of cells were captured as digital images and measured with image analysis software (Image J; National Institutes of Health, Bethesda, MD). Labeling with Calcein AM (Sigma-Aldrich, St Louis, MO) was used to delineate the plasma membrane of sNF96.2 and sNF02.2 cells from the indistinct pericellular matrix after treatment with 1.0 mM MU. The cells were photographed using a Keyence inverted phase-contrast fluorescence microscope. The proportion of pericellular matrix areas to cell areas was evaluated as described previously.[15] A matrix area was defined by the area delineated by the pericellular matrix minus the area delineated by the plasma membrane (defined as cell area). In the absence of detectable matrices, the matrix/cell ratio would be 0.0.

183

184 Quantification of HA

185 Both sNF96.2 and sNF02.2 cells were incubated with (1.0 mM MU) or without
186 MU (0.1% DMSO) for 12 h and 24 h. HA was isolated according to previously described
187 methods.[30] Briefly, the conditioned medium was collected and designated as “medium”.
188 To extract the cell-surface associated HA, the cells were incubated for 10 min at 37 °C
189 with trypsin-EDTA and washed with PBS. The trypsin solution and combined washes
190 were designated as “pericellular.” After cell counting, the cells were placed in
191 Proteinase K solution (0.15 M Tris–HCl, pH 7.5, 0.15 M NaCl, 0.01 M $CaCl_2$, and 5 mM
192 deferoxamine mesylate containing 20 U of proteinase K) and incubated for 2 h at 55 °C,
193 and this solution was designated as “intracellular.” All samples were heated at 100 °C
194 for 15 min to inactivate protease activity and centrifuged at 15,000g for 30 min at 4 °C,
195 after which the supernatants were analyzed. The HA concentrations were measured
196 using the HA binding assay, as described previously.[31] Briefly, each well in a Maxisorp
197 microtiter plate (Nunc, Roskilde, Denmark) was coated with 50 µl of HABP (Seikagaku,
198 Tokyo, Japan; 0.4 µg/ml in 0.1 M NaHCO3, pH9.2), overnight at 4°C, and subjected to
199 blocking with 200 µl each of 2% BSA in phosphate-buffered saline with 0.1% (v/v)
200 Tween 20 (PBS-T) at room temperature for 2 h. After washing with PBS-T, samples (50
201 µl each) or standard HA solutions were applied, and the wells were incubated at 37°C
202 for 1 h. After washing, 50 µl of biotinylated HABP (Seikagaku, Tokyo, Japan; 0.3 µg/ml,
203 diluted with 1% BSA/PBS-T) was added, and the plate was incubated at 37°C for 1 h.
204 Subsequently, peroxidase-conjugated streptavidin (Jackson Immuno Research
205 Laboratories; diluted 1:2,000 with 1% BSA/PBS-T) was applied (50 µl each) for 1 h at
206 37°C. After incubation with 50 µl of 3,30,5,50-tetramethylbenzidine substrate (KPL,
207 Gaithesburg, CA) at 37°C for 10 min., the absorbance at 450 nm was measured on a
208 VERSA max microplate reader (Molecular Devices, Sunnyvale, CA).

209

210 Cell proliferation assay

211 Both sNF96.2 and sNF02.2 cells (1×10^4 /well) were seeded in 96-well plates
212 with 10% FBS. The cells were treated with (0.1 mM and 1.0 mM) or without MU (0.1%
213 DMSO). Following 24 h, 48 h, and 72 h of treatment, cell proliferation was assessed
214 with a Cell Counting Kit 8 (Dojindo Laboratories, Kumamoto, Japan). The plates were
215 incubated for 1 h after the addition of the reagent, and the absorbance was measured at
216 490nm with a microplate reader (Tecan Sunrise; Tecan Inc, Mannedorf, Switzerland).
217 Microscopic inspection of the wells confirmed that decreased absorbance values
218 correlated with decreased cell number. We also investigated whether exogenously
219 added high-molecular weight hyaluronan (HMWHA, 600–1,200 kDa, Seikagaku, Tokyo,
220 Japan) could inhibit the effects of MU. MPNST cells were incubated with 0–1.0 mM
221 MU with or without 200 μg/ml of HMWHA for 24, 48, and 72 h.

222

223 Cell migration and invasion assays

224 Chemotactic motility of sNF96.2 and sNF02.2 cells was investigated using 12-well
225 cell culture chambers containing inserts with 12-μm pores (Millipore, Billerica, MA)
226 after 24 h of treatment with (0.1 mM and 1.0 mM) or without MU (0.1% DMSO).
227 Invasiveness of MPNST cells was evaluated in the same chambers which contain the
228 inserts with a 12-μm pore membrane coated with 100 μg/ml matrigel. The cells were
229 added to the upper chamber at a density of 5×10^5 cells/insert in the presence or
230 absence of MU (0.1 mM and 1.0 mM) with or without 200 μg/ml of HMWHA, and
231 chemotactic medium containing 10% FBS was placed in the lower chamber. After
232 incubation for 24 h, the cells on the upper side of each membrane were removed by
233 wiping with cotton swabs. The cells on the lower surface of the membrane were fixed
234 with 70% ethanol and stained with hematoxylin. The cell numbers of 10 different fields

on the lower side were counted under a light microscope (magnification × 200).

In addition, to determine whether the effects of MU are mediated by the function of CD44, a key HA receptor, the migratory activity and invasiveness of sNF96.2 and sNF02.2 cells treated with MU were evaluated after knockdown of CD44 using siRNAs. Briefly, siRNA for Hyaluronic acid receptor cell adhesion molecule (HCAM; Santa Cruz Biotechnology, Santa Cruz, CA) were complexed with Lipofectamine RNAiMAX (Invitrogen, Carlsbad, CA) in Opti-MEM (Gibco, Life technologies) according to the manufacturer's instruction, and then the mixtures were administered to sNF96.2 and sNF02.2 cells in DMEM with serum and antibiotics. As a control siRNA, the Silencer negative control (Ambion, Austin, TX) was used. For 48-h incubation, efficiency of knockdown with siRNA for CD44 was confirmed using real-time RT-PCR. The effects of MU on cell migration and invasion were analyzed under the condition of CD44 knockdown.

Evaluation for cell apoptosis

We examined whether the growth inhibition by MU was attributable to the induction of apoptosis. The effects of MU on cell apoptosis were measured by flow cytometry with anti-Annexin V antibody after incubation for 48 h with (0.1 mM and 1.0 mM) or without MU (0.1% DMSO). Both sNF96.2 and sNF02.2 cells were harvested and washed with PBS. Annexin V-FITC and binding buffer (Annexin V-FITC Apoptosis Detection Kit Plus; BioVision, Milpitas, CA) were added to the cells and incubated on ice for 15 min in the dark. After incubation, binding buffer was applied to each tube. Data were analyzed with FACS Calibur (Becton Dickinson, San Jose, CA) and Flow-Jo 7 software (Tree Star, Ashland, OR). To investigate the time-course effects of MU on apoptotic activity of sNF96.2 and sNF02.2 cells, TUNEL (TdT: terminal deoxynucleotidyltransferase-mediated dUTP nick end labeling) staining was carried

261 out at different periods of time (24, 72, and 96 h). The subconfluent cells were
262 incubated with (0.1 mM and 1.0 mM) or without MU (0.1% DMSO) for 24, 48, 72, and
263 96 h, and subjected to TUNEL staining using an In Situ Cell Death Detection Kit, POD
264 (Roche Diagnostics, Mannheim, Germany). Cells with brown-stained nuclei in 10
265 different fields were counted under a light microscope (magnification × 200), and the
266 percentage of positive-staining cells was calculated, and compared with control culture
267 with the medium containing 0.1% DMSO.
268
269 Real-time RT-PCR
270 Both sNF96.2 and sNF02.2 cells were treated with (0.1 mM and 1.0 mM) or
271 without MU (0.1% DMSO) for 6, 12, and 24 h. Total RNA was extracted with RNeasy
272 Micro kit (Qiagen, San Diego, CA). Reverse-transcribed cDNA was subjected to real
273 time RT-PCR for semi-quantification of HAS1, HAS2, HAS3, and CD44 mRNAs using a
274 Light-Cycler (Roche Diagnostics, Mannheim, Germany). The relative expression levels
275 of HASs and CD44 mRNAs of sNF96.2 and sNF02.2 cells were normalized with
276 GAPDH mRNA levels. Specific oligonucleotide primer pairs were HAS1 (forward, 5'-
277 CAGACCCACTGCGATGAGAC-3'; reverse, 5'-CCACCAGGTGCGCTGAAA-3)', HAS2
278 (forward, 5'-TCAGAGCACTGGGACGAAG-3' ; reverse, 5'-CCCAACACCTCCAACCCAT-
279 3'), HAS3 (forward, 5'-CAGCAACTTCCAATGAGGC-3' ; reverse, 5'-
280 CACAGTGTCAGAGTCGCA-3'), CD44 (forward, 5'-CTGAGCCTGGCGCAGATCG-3' ;
281 reverse, 5'-CCTCCGTCCGAGAGATGCTG-3'), and human GAPDH (forward, 5'-
282 TGCACCACCAACTGCTTAGC-3' ; reverse, 5'-GGCATGGACTGTGGTCATGAG-3'). The
283 mRNA level at each time point was shown as a ratio to the control cultures with the
284 medium containing 0.1% DMSO.
285
286 MPNST xenograft model

Animal experiments were approved by the Animal Research Committee of our institution. Six-week-old female athymic nude mice (BALB/C nu/nu mice; SLC, Shizuoka, Japan) were used in this study. To establish the xenograft model, two human MPNST cell lines, sNF96.2 and sNF02.2, were injected subcutaneously into the flanks of the mice at a concentration of 2×10^7 cells in 200 μl suspension of PBS. Tumors routinely developed in mice injected with sNF96.2 cells, but not with sNF02.2 cells. For *in vivo* passage, the developed sNF96.2 tumors were harvested from the mice, minced in PBS by homogenization at lowest speed, and 100 μl of homogenized solution was re-implanted into the flank of other tumor-naive mice according to the protocol described by Faltz et al.[32] When implanted tumor volumes reached approximately 100 mm^3, mice were randomized into two groups (n = 8 each). In the MU-treated group, MU (10 mg/body weight; approximately equal to 400-500mg/kg) dissolved in 100 μl of 0.4% carboxymethylcellulose (CMC) solution (Sigma-Aldrich, St Louis, MO) was administered intraperitoneally daily for six weeks. We previously reported that systemic administration of MU (10mg/body weight; 400-500mg/kg) did not affect the structure of normal skin, articular cartilage and body weight in mouse bone metastasis model[23]. In the control group, the same amount of 0.4% CMC solution without MU was administered intraperitoneally to the mice for six weeks. Tumors were monitored twice a week. Tumor size was determined with a caliper, and the volume was calculated by the formula V (mm^3) = [length (mm)] × [width (mm)]^2 × 0.5. All tumors were resected after the treatment for six weeks.

Immunohistochemical staining for Ki67

Ki67 protein is widely known as an appropriate and useful marker of the proliferating fraction within a given cell population. We performed Ki67 immunostaining for xenograft tumors to examine the effects of MU on the proliferation

313 *in vivo*. Deparaffinized and rehydrated sections were treated with 0.3% H_2O_2 in
314 methanol for 30 min to block the internal peroxidase activity. The sections were
315 incubated with mouse anti-human Ki67 monoclonal antibody (Dako, Glostrup,
316 Denmark) as a primary antibody (dilution; 1:500) using Histofine MOUSESTAIN KIT
317 (Nichirei, Tokyo, Japan) according to the manufacturer's instructions. Biotinylated
318 anti-mouse goat IgG (Nichirei, Tokyo, Japan) was applied as a secondary antibody for
319 30 min at room temperature, and antibody binding was detected by the addition of
320 streptavidin-peroxidase reagents and diaminobenzidine-containing substrate solution
321 (Nichirei, Tokyo, Japan). Five fields (magnification × 400) were randomly selected in
322 each section. Ki67-positive cells of these fields were counted and divided by the total
323 number of tumor cells in each field. Three tumors each from the control and MU-
324 treated mice were analyzed.
325
326 Statistical analysis
327 All the quantitative experiments *in vitro* were performed more than three times.
328 Bonferroni–Dunn post hoc test was used to assess the differences between means in
329 multiple groups, and Mann–Whitney U test or Student's *t* test were used to distinguish
330 differences between two groups. P values of less than 0.05 were considered statistically
331 significant.
332
333 **Results**
334 HA staining in cells
335 Both sNF96.2 and sNF02.2 cells treated with the control medium (0.1% DMSO)
336 without MU for 24 h showed prominent staining for HA in cytoplasms of tumor cells
337 (Fig. 1a). The positivity for HA was decreased, but not completely abrogated after 24-h
338 treatment with 1.0 mM MU in both MPNST cell lines. The MU treatment caused

morphological change of cells, particularly reduced formation of cell processes and filopodia-like structures in sNF02.2, as compared with the cells treated with control cultures (0.1% DMSO) (arrowheads, Fig. 1a).

Particle exclusion assay

As shown in Fig. 1b, both sNF96.2 and sNF02.2 cells treated with control cultures (0.1% DMSO) showed abundant pericellular matrices (halo area around the cells; arrows) after incubation for 48 h. The treatment with 1.0 mM MU resulted in a substantial decrease in the area of pericellular matrices in both cell lines. Staining with Calcein AM enabled to define pericellular matrices treated with the control culture, and a loss of pericellular matrix treated with 1.0 mM MU surrounding both sNF96.2 and sNF02.2 cells. The ratio of pericellular matrix areas to cell areas in both cell lines treated with 1.0 mM MU was significantly lower than those treated with control cultures (0.1% DMSO) (sNF96.2; $P = 0.001$ and sNF02.2; $P = 0.002$, respectively; Fig. 1c).

Quantification of pericellular HA

The amount of HA (ng) was measured per 10^5 cells each in sNF96.2 and sNF02.2 cells, using the HA binding assay. As shown in Fig. 2, at the 12- and 24-h time points of cell culture, 1.0 mM MU significantly suppressed the amount of intracellular and pericellular HA in both sNF96.2 and sNF02.2 cells. The amount of HA in medium was also significantly decreased after 12- and 24-h treatment with 1.0 mM MU in both sNF96.2 and sNF02.2 cells, respectively.

Cell proliferation

Preliminary experiments revealed that cell viability of each cell line incubated

365 with 1.0 mM MU for 24- and 48-h was more than 95 % by Trypan Blue Exclusion assay.
366 Treatment with 0.1 mM and 1.0 mM MU significantly inhibited the proliferation of
367 sNF96.2 and sNF02.2 cells in a dose- and time-dependent manner, compared with the
368 cells treated without MU (Fig. 3a and 3b, respectively). Even with a concentration of
369 0.1 mM MU treatment, cell proliferation was significantly reduced. Maximal reduction
370 was obtained at a concentration of 1.0 mM in both sNF96.2 and sNF02.2 cells.
371 Exogenously added HMWHA did not recover the inhibition of cell proliferation by MU
372 in both MPNST cells.
373
374 Cell migration and invasion assays
375 At the 24-h time point of cell culture, the migratory activity of sNF96.2 and
376 sNF02.2 cells treated with 1.0 mM MU was significantly suppressed compared with the
377 cells with control cultures (0.1% DMSO) ($P < 0.001$ and $P < 0.001$, respectively; Fig. 3c).
378 Treatment with 0.1 mM MU did not exhibit a statistically significant reduction
379 compared with the cells treated with the control cultures (0.1% DMSO) in migratory
380 activity of either MPNST cell lines. Invasiveness of sNF96.2 and sNF02.2 cells treated
381 with 1.0 mM MU was significantly lower than that of the cells treated with the control
382 cultures (0.1% DMSO) ($P < 0.001$ and $P < 0.001$, respectively; Fig. 3d). Treatment with
383 0.1 mM MU significantly suppressed the invasiveness of sNF02.2 cells compared with
384 that of the control cultures (0.1% DMSO) ($P < 0.001$; Fig. 3d). Exogenously added
385 HMWHA did not recover the suppressed migratory activity and invasiveness by MU in
386 sNF96.2 and sNF02.2 cells.
387
388 Apoptosis assay
389 Flow cytometric analysis of Annexin V, an early apoptotic cell marker, showed
390 that 1.0 mM MU significantly induced more apoptosis in sNF96.2 cells ($P = 0.001$; Fig.

391 3e), whereas apoptosis was not induced by MU treatment in sNF02.2 cells, even at a
392 dose of 1.0 mM. At the 48-h time points of cell culture, the apoptotic activity of cells
393 treated with MU varied between the two MPNST cell lines [Supplementary Fig. 1a (i–
394 vi)]. TUNEL staining was also used to evaluate the apoptotic effect of MU on MPNST
395 cells at different periods of time. Treatment with 1.0 mM MU significantly increased
396 the ratio of apoptotic cells at each time point in sNF96.2 cells (24 h; $P = 0.001$, 48 h; $P =$
397 0.044, 72 h; $P = 0.001$, and 96 h; $P = 0.002$, respectively; Supplementary Fig. 1b), and at
398 the 72- and 96-h time point in sNF02.2 cells (72 h; $P = 0.006$ and 96 h; $P = 0.005$,
399 respectively). As a definitive positive control of MU effects on apoptosis, a human
400 breast cancer cell line, MDA-MB-231 cells, were used, which were reported to increase
401 apoptotic activity with MU treatment[23]. The results of the present study was consistent
402 with the previous ones that positivity of TUNEL staining in MDA-MB-231 cells
403 significantly increase after 72-h treatment with 0.1 and 1.0 mM MU.
404
405 Real time RT-PCR
406 To determine the effects of MU on HA synthesis at messenger levels in human
407 MPNST cells, HAS1-3 and CD44 mRNA expression was analyzed. HAS1 mRNA was
408 undetectable by RT-PCR in both sNF96.2 and sNF02.2 cell lines (data not shown), and
409 so we determined the HAS2, HAS3, and CD44 mRNA levels in sNF96.2 and sNF02.2
410 cells. Treatment with 1.0mM MU for 12 h significantly reduced mRNA expression of
411 HAS2 in both sNF96.2 and sNF02.2 cell lines compared with that in the control
412 cultures ($P < 0.001$ and $P = 0.009$, respectively; Fig. 3f). Expression levels of HAS3
413 mRNA in sNF96.2 cells treated with 0.1 mM and 1.0 mM MU were significantly
414 downregulated compared with those in the control cultures ($P < 0.001$ and $P < 0.001$;
415 respectively, Fig. 3g). In sNF02.2 cells, HAS3 mRNA was also decreased by MU in a
416 dose-dependent manner, with the reduction, however, not reaching statistical

significance (Fig. 3g). Time-course analyses revealed that 1.0 mM MU significantly reduced mRNA expression of HAS2 in both MPNST cell lines at every time point, except at 24 h of sNF96.2 cells. Expression levels of HAS3 mRNA were downregulated in a time-dependent manner by 0.1 mM and/or 1.0 mM MU in sNF96.2 cells and sNF02.2 cells (Supplementary Fig. 2). Expression level of CD44 mRNA in sNF96.2 cells and sNF02.2 cells treated with 0.1 mM or 1.0 mM MU varied according to periods of incubation and types of cell lines. (Supplementary Fig. 2).

Knockdown of CD44

To investigate whether a main hyaluronan receptor, CD44, affect the results of MU treatment, effects of siRNA knockdown for CD44 on tumorigenicity in sNF96.2 and sNF02.2 cells were evaluated. After knockdown, CD44 mRNA expression was decreased to less than 10 % of control siRNA in both cell lines. Interestingly, CD44 knockdown itself had inhibitory effects of cell migration and invasiveness in both cell lines. Co-treatment of siRNA CD44 and MU had additive inhibitory effects of migration and invasion in sNF96.2 and sNF02.2 cells (Supplementary Fig. 3). However, these results could not conclude that MU effects are mediated by CD44 or not.

Tumor growth in the xenograft model

Two human MPNST cell lines, sNF96.2 and sNF02.2, were injected in the flank of nude mice. *In vivo* tumorigenicity was confirmed only in sNF96.2 cell injected mice. Daily administration of MU (10 mg/body weight) for six weeks significantly suppressed the increase of tumor volume of sNF96.2 compared with that with control treatment (4W; $P = 0.007$, 5W; $P = 0.074$, and 6W; $P = 0.006$, respectively; Fig. 4a) and tumor weight ($P = 0.047$; Fig.4b), as compared with those of the control mice treated with a vehicle (Fig. 4c). Positivity for HA of tumor cells and stromal tissues was suppressed

443 with MU treatment [Fig. 4d (i–iv)]. Immunostaining of Ki67, which is a marker for cell
444 proliferation, revealed that the ratio of Ki67-positive cells in tumor cells of MU-treated
445 mice was significantly reduced compared to that of vehicle-treated mice[Fig. 4d (v–vi)]
446 (P = 0.002, Fig. 4e). The body weight of mice was measured twice a week during the
447 drug administration. There was no statistical difference in body weight between the
448 mice treated and untreated with MU at each time point (Fig. 4f). Body weight
449 excluding tumor weight also did not differ between the control and MU-treated mice
450 after the treatment for six weeks (P = 0.147).
451
452
453 **Discussion**
454 In general, the clinical outcome of patients with advanced MPNST is dismal.
455 Doxorubicin and ifosfamide are currently the most active chemotherapeutic agents in
456 patients with unresectable and metastatic soft tissue sarcomas; however, the Response
457 Evaluation Criteria in Solid Tumors (RECIST) response rate for the combination is
458 reported to be only approximately 26%.[33] The responses were no better in patients with
459 MPNST, shown to be 21% in a multi-institution retrospective study for patients with
460 unresectable and metastatic MPNST.[34] A novel therapeutic tool other than existing
461 chemotherapeutic agents is thus urgently required to improve the prognosis of patients
462 with advanced MPNST.
463 Recently, Slomiany et al. reported that HA oligomers suppressed HA secretion in
464 MPNST cells, decreased doxorubicin resistance of MPNST, and suppressed the growth
465 of MPNST xenografts in mice, which implicated the importance of HA in the
466 tumorigenicity of MPNST.[35] Our previous study demonstrated that increased HA
467 expression in MPNST tissues significantly correlated with poor prognosis in patients
468 with MPNST.[26] Based on these results, there is a great need to identify pharmacologic

agents that effectively inhibit HA synthesis for MPNST, and are also clinically applicable.

Several studies have shown the antitumor effects of MU in various malignancies mediated by inhibition of HA synthesis.[19–25, 36–38] It was reported that the inhibitory effects of MU on cell migration and invasion could be explained by inhibition of extracellular matrix formation through inhibition of HA synthesis in several cancer cell lines.[19,23,24,39] However, these studies examined the antitumor effect of MU primarily focused on cancer cells of epithelial origin. The behavior of mesenchymal cells may differ from that of epithelial cells because mesenchymal cells likely have more abundant HA-rich matrices compared with epithelial cells. The antitumor effects of MU in mesenchymal malignancies appeared to differ from those in epithelial malignancies. The results of the particle exclusion assay in the present study revealed that MPNST cells had abundant pericellular matrices, which were larger than the pericellular matrix formation previously reported in cancer cells such as melanoma and pancreatic cancer cells.[19,22] Previous studies described that the inhibition of pericellular matrices via inhibition of HA accumulation resulted in reduced tumorigenicity of osteosarcoma cells. [14,15] In our study, MU treatment significantly decreased the amount of pericellular matrices concurrently with the reduction of the concentrations of intracellular and pericellular HA determined with HA binding assay in both sNF96.2 and sNF02.2 cells. These results implied that the depletion of pericellular matrix formation might be partly attributable to the depletion of HA by MU treatment in MPNST cells. Furthermore, HA staining *in vitro* revealed that MU inhibited accumulation of pericellular HA in MPNST cells, and diminished the filopodia-like structure after MU treatment in the present study, which was consistent with a previous report.[23] These suggest that morphological change of cells possibly induced by HA depletion with MU treatment might contribute in a significant way to the inhibition of tumorigenicity. On

the other hand, exogenously added HA could not cancel the effects of MU in the present study, which is inconsistent with the results in prostate cancer cells[21]. Newly synthesized HA bound to the HA synthase complex rather than non-bound HA in extracellular matrix might be important to maintain tumorigenicity of MPNST.

MU was reported to suppress mRNA levels of HAS2 and/or HAS3 in several carcinoma cell lines in a dose-dependent manner.[20,21,23] Kultti et al. reported that a dose-dependent reduction by MU in the mRNA levels of HAS2 or HAS3, or both, was detected in four different cancer cell lines, and that alterations of the mRNA levels depended on the kind of tumor.[20] Results of these reports are consistent with the findings of our study with sNF96.2 and sNF02.2 cells, in which HAS2 and HAS3 mRNA levels were downregulated after treatment with MU. On the other hand, other researchers have demonstrated a significant contribution of HAS2 and HAS3 to the tumorigenicity of malignant cells. Kosaki et al. showed that Has2 transfection in HT1080 cells, a human fibrosarocma cell line, resulted in increased HA production, tumor cell proliferation, and tumor size in xenograft models.[40] Li et al. described that siRNA-mediated knockdown of HAS2 suppressed cell growth and cellular migratory and invasive potential in human breast cancer cells.[17] Taken together with the results of these previous studies, MU was thought to inhibit the tumorigenicity of MPNST cells partly through repression of HAS2 and/or HAS3 mRNA in the present study. However, it has not yet been elucidated how MU downregulated the levels of HASs mRNA at the molecular level.

In the present study, the proliferation of sNF96.2 and sNF02.2 cells was significantly suppressed by MU, supporting previous data on other types of tumor cell.[15,20–24,36] The apoptotic activity of sNF96.2 cells was induced by MU treatment, whereas that of sNF02.2 was not. Recent studies demonstrated that MU treatment was associated with growth arrest and apoptosis of tumor cells,[21,23,37] whereas Edward et al. reported that

MU had no effect on apoptosis of melanoma cells,[38] suggesting that stimulation of apoptosis may be tumor-type dependent, and/or vary among cell lines of the same malignant neoplasms.

The current study also examined the antitumor effects of MU in a xenograft model of MPNST. Tumors developed in the sNF96.2 cell transplanted mice, but not in sNF02.2 cell transplanted ones. Considering that sNF96.2 cells were derived from locally recurrent MPNST and sNF02.2 cells from metastatic MPNST of lung, a possible explanation was that the affinity of these cells for host tissues of mice ("seed and soil" theory) might affect the establishment of xenograft tumors. Another explanation might be that MPNST is a group of extremely heterogeneous tumors, particularly with regard to their genomic alterations, which will affect the development of tumors *in vivo*. Our previous report investigating HASs expression in human MPNST tissues showed that expression patterns of HAS1, 2, and 3 were markedly heterogeneous among cases.[26] MU significantly reduced the growth rate of sNF96.2 tumors in the xenograft model, possibly mediated by reduced deposition of HA in tumorous and stromal tissues. MU could not show the effects of tumor shrinkage, but have "tumor-dormancy" effects for MPNST.

The molecular mechanisms underlying MPNST development and progression are not fully understood. Although several preclinical studies are underway to develop a targeted therapy for MPNST based on molecular approaches, successful results of clinical trials with novel agents are absent. Since NF1 gene product, neurofibromin, acts as a negative regulator in the Ras signal transduction pathway, several studies evaluating potential treatments for MPNST have focused on the compounds that block Ras signaling, such as farnesyl transferase inhibitors or mTOR inhibitors.[41–43] Other studies have investigated targeted therapies for molecules such as erlotinib (EGFR inhibitor), sorafenib (VEGFR and RAF inhibitor), and imatinib mesylate (tyrosine-

kinase inhibitor).[44–46] These compounds have shown positive effects *in vitro* and/or in *in vivo* studies, while demonstrating a limitation as a single agent in human clinical trials.[47–51] It is suggested that a major problem of a target therapy for signal pathways may be the capability of tumor cells to mutate and use alternate pathways for survival and proliferation thereby escaping specific inhibitor action. “Second hits” other than NF1 mutation vary among MPNSTs, making it difficult to target a single pathway for therapy of MPNSTs. Therefore, additional therapeutic approaches relying on other antitumor mechanisms are more likely to be needed in patients with MPNST.

MU is already an established therapeutic agent for choleretic and biliary antispasmodic activity.[25] The clinical experience to date also reveals that MU is a safe and well-tolerated oral medication. Our results showed that MU suppressed cell growth *in vitro* and *in vivo*, increased apoptosis activity, and attenuated cell migration and invasion of MPNST through the inhibition of HA synthesis and possibly alteration of the tumor microenvironment. Although further investigations are warranted to clarify the efficacy and mechanisms of MU in patients with MPNST, HA-targeting therapy with MU may have potential as a novel therapeutic tool for patients with MPNST.

Acknowledgements

We thank Ms. Eri Ishihara for secretarial assistance for the experiments. This work was supported in part by the National Cancer Center Research and Development Fund (26-A-4), and the Ministry of Education, Culture, Sports, Science and Technology of Japan [Grant-in-Aid 15K19992 for Young Scientists (B)].

Declaration of interest

The authors report no conflicts of interest.

References

1. Goldblum JR, Folpe AL, Weiss SW. Malignant tumors of the peripheral nerves. In: Goldblum JR, Folpe AL, Weiss SW. Enzinger and Weiss's Soft tissue tumors, 6th ed. Philadelphia: Elsevier, 2014. 855–879

2. McGaughran, JM, Harris, DI, Donnai D, Teare D, MacLeod R, Westerbeek R, Kingston H, Super M, Harris R, Evans DG. A clinical study of type 1 neurofibromatosis in North West England. J Med Genet 1999; 36: 197–203

3. Katz D, Lazar A, Lev D. Malignant peripheral nerve sheath tumor (MPNST): the clinical implications of cellular signalling pathways. Expert Rev Mol Med 2009; 11: e30

4. Itano N, Sawai T, Yoshida M, Lenas P, Yamada Y, Imagawa M, Shinomura T, Hamaguchi M, Yoshida Y, Ohnuki Y, Miyauchi S, Spicer AP, McDonald JA, Kimata K. Three isoforms of mammalian hyaluronan synthases have distinct enzymatic properties. J Biol Chem 1999; 274: 25085–92

5. Knudson CB, Knudson W. Hyaluronan-binding proteins in development, tissue homeostasis, and disease. FASEB J 1993; 7: 1233–41

6. Turley E, Noble PW, Bourguignon LYW. Signaling properties of hyaluronan receptors. J Biol Chem 2002; 277: 4589–92

7. Toole BP. Hyaluronan: from extracellular glue to pericellular cue. Nat Rev Cancer 2004; 4: 528–39

8. Anttila MA, Tammi RH, Tammi MI, Syrjänen KJ, Saarikoski SV, Kosma VM. High Levels of Stromal Hyaluronan Predict Poor Disease Outcome in Epithelial Ovarian Cancer. Cancer Res 2000; 60: 150–5

9. Pirinen R, Tammi R, Tammi M, Hirvikoski P, Parkkinen JJ, Johansson R, Böhm J,

597 Hollmen S, Kosma VM. Prognostic value of hyaluronan expression in non-small-cell
598 lung cancer: Increased stromal expression indicates unfavorable outcome in patients
599 with adenocarcinoma. Int J Cancer 2001; 95: 12–7

600 10. Böhm J, Niskanen L, Tammi R, Tammi M, Eskelinen M, Prinen R, Hollmen S,
601 Alhava E, Kosma VM. Hyaluronan expression in differentiated thyroid carcinoma. J
602 Pathol 2002; 196: 180–5

603 11. Auvinen P, Tammi R, Parkkinen J, Tammi M, Agren U, Johansson R, Hirvikoski P,
604 Eskelinen M, Kosma VM. Hyaluronan in peritumoral stroma and malignant cells
605 associates with breast cancer spreading and predicts survival. Am J Pathol 2000; 156:
606 529–36

607 12. Ropponen K, Tammi M, Parkkinen J, Eskelinen M, Tammi R, Lipponen P, Agren U,
608 Alhava E, Kosma VM. Tumor Cell-associated Hyaluronan as an Unfavorable Prognostic
609 Factor in Colorectal Cancer. Cancer Res 1998; 342–7

610 13. Setälä LP, Tammi MI, Tammi RH, Eskelinen MJ, Lipponen PK, Agren UM, Alhava
611 EM, Kosma VM. Hyaluronan expression in gastric cancer cells is associated with local
612 and nodal spread and reduced survival rate. Br J Cancer 1999; 79: 1133–8

613 14. Nishida Y, Knudson W, Knudson CB Ishiguro N. Antisense inhibition of hyaluronan
614 synthase-2 in human osteosarcoma cells inhibits hyaluronan retention and
615 tumorigenicity. Exp Cell Res 2005; 307: 194–203

616 15. Arai E, Nishida Y, Wasa J, Urakawa H, Zhuo L, Kimata K, Kozawa E, Futamura N,
617 Ishiguro N. Inhibition of hyaluronan retention by 4-methylumbelliferone suppresses
618 osteosarcoma cells in vitro and lung metastasis in vivo. Br J Cancer 2011; 105: 1839–49

619 16. Udabage L, Brownlee GR, Waltham M, Blick T, Walker EC, Heldin P, Nilsson SK,
620 Thompson EW, Brown TJ. Antisense-Mediated Suppression of Hyaluronan Synthase 2

621 Inhibits the Tumorigenesis and Progression of Breast Cancer. Cancer Res 2005; 65:
622 6139–51.

623 17. Li Y, Li L, Brown TJ, Heldin P. Silencing of hyaluronan synthase 2 suppresses the
624 malignant phenotype of invasive breast cancer cells. Int J Cancer 2007; 120: 2557–67

625 18. Kakizaki I, Kojima K, Takagaki K, Endo M, Kannagi R, Ito M, Maruo Y, Sato H,
626 Yasuda T, Mita S, Kimata K, Itano N. A novel mechanism for the inhibition of
627 hyaluronan biosynthesis by 4-methylumbelliferone. J Biol Chem 2004; 279: 33281–9

628 19. Kudo D, Kon A, Yoshihara S, Kakizaki I, Sasaki M, Endo M, Takagaki K. Effect of a
629 hyaluronan synthase suppressor, 4-methylumbelliferone, on B16F-10 melanoma cell
630 adhesion and locomotion. Biochem Biophys Res Commun 2004; 321: 783–7

631 20. Kultti A, Pasonen-Seppänen S, Jauhiainen M, Rilla KJ, Kärnä R, Pyöriä E, Tammi
632 RH, Tammi MI. 4-Methylumbelliferone inhibits hyaluronan synthesis by depletion of
633 cellular UDP-glucuronic acid and downregulation of hyaluronan synthase 2 and 3. Exp
634 Cell Res 2009; 315: 1914–23

635 21. Lokeshwar VB, Lopez LE, Munoz D, Chi A, Shirodkar SP, Lokeshwar SD, Escudero
636 DO, Dhir N, Altman N. Antitumor activity of hyaluronic acid synthesis inhibitor 4-
637 methylumbelliferone in prostate cancer cells. Cancer Res 2010; 70: 2613–23

638 22. Nakazawa H, Yoshihara S, Kudo D, Morohashi H, Kakizaki I, Kon A, Takagaki K,
639 Sasaki M. 4-methylumbelliferone, a hyaluronan synthase suppressor, enhances the
640 anticancer activity of gemcitabine in human pancreatic cancer cells. Cancer Chemother
641 Pharmacol 2006; 57: 165–70

642 23. Urakawa H, Nishida Y, Wasa J, Arai E, Zhuo L, Kimata K, Kozawa E, Futamura N,
643 Ishiguro N. Inhibition of hyaluronan synthesis in breast cancer cells by 4-
644 methylumbelliferone suppresses tumorigenicity in vitro and metastatic lesions of bone

645 in vivo. Int J Cancer 2012; 130: 454–66

646 24. Futamura N, Urakawa H, Arai E, Kozawa E, Ishiguro N, Nishida Y. Hyaluronan
647 synthesis inhibitor supplements the inhibitory effects of zoledronic acid on bone
648 metastasis of lung cancer. Clin Exp Metastasis 2013; 30: 595–606

649 25. Nagy N, Kuipers HF, Frymoyer AR, Ishak HD, Bollyky JB, Wight TN, Bollyky PLet
650 al. 4-Methylumbelliferone Treatment and Hyaluronan Inhibition as a Therapeutic
651 Strategy in Inflammation, Autoimmunity, and Cancer. Front Immunol 2015; 6: 1–11

652 26. Ikuta K, Urakawa H, Kozawa E, Arai E, Zhuo L, Futamura N, Hamada S, Kimata
653 K, Ishiguro N, Nishida Y. Hyaluronan expression as a significant prognostic factor in
654 patients with malignant peripheral nerve sheath tumors. Clin Exp Metastasis 2014; 31:
655 715–25

656 27. Nishida Y, Knudson CB, Nietfeld JJ, Margulis A, Knudson W. Antisense inhibition
657 of hyaluronan synthase-2 in human articular chondrocytes inhibits proteoglycan
658 retention and matrix assembly. J Biol Chem 1999; 274: 21893–9

659 28. Nishida Y, D'Souza AL, Thonar EJ, Knudson W. Stimulation of hyaluronan
660 metabolism by interleukin-1alpha in human articular cartilage. Arthritis Rheum. 2000;
661 43: 1315–26

662 29. Nishida Y, Knudson CB, Knudson W. Osteogenic protein-1 inhibits matrix depletion
663 in a hyaluronan hexasaccharide-induced model of osteoarthritis. Osteoarthr Cartil
664 2004; 12: 374–82

665 30. Tammi R, Rilla K, Pienimäki JP, MacCallum DK, Hogg M, Luukkonen M, Hascall
666 VC, Tammi M. Hyaluronan Enters Keratinocytes by a Novel Endocytic Route for
667 Catabolism. J Biol Chem 2001; 276: 35111–22

668 31. Zhu L, Zhuo L, Kimata K, Yamaguchi E, Watanabe H, Aronica MA, Hascall VC,

669 Baba K. Deficiency in the serum-derived hyaluronan-associated protein-hyaluronan
670 complex enhances airway hyperresponsiveness in a murine model of asthma. Int Arch
671 Allergy Immunol 2010; 153: 223–33

672 32. Faltz LL, Reddi AH, Hascall GK, Martin D, Hascall VC. Characteristics
673 Chondrosarcoma of proteoglycans extracted from the Swarm rat chondrosarcoma with
674 associative solvents. J Biol Chem 1979; 254:1375–80

675 33. Judson I, Verweij J, Gelderblom H, Hartmann JT, Schöffski P, Blay JY, Kerst JM,
676 Sufliarsky J, Whelan J, Hohenberger P, Krarup-Hansen A, Alcindor T, Marreaud S,
677 Litière S, Hermans C, Fisher C, Hogendoorn PC, dei Tos AP, van der Graaf WT.
678 Doxorubicin alone versus intensified doxorubicin plus ifosfamide for first-line
679 treatment of advanced or metastatic soft-tissue sarcoma: A randomised controlled
680 phase 3 trial. Lancet Oncol 2014; 15: 415–23.

681 34. Kroep JR, Ouali M, Gelderblom H, Le Cesne A, Dekker TJ, Van Glabbeke M,
682 Hogendoorn PCW, Hohenberger P. First-line chemotherapy for malignant peripheral
683 nerve sheath tumor (MPNST) versus other histological soft tissue sarcoma subtypes
684 and as a prognostic factor for MPNST: An EORTC Soft Tissue and Bone Sarcoma Group
685 study. Ann Oncol 2011; 22: 207–14

686 35. Slomiany MG, Dai L, Bomar PA, Knackstedt TJ, Kranc DA, Tolliver L, Maria BL,
687 Toole BP. Abrogating drug resistance in malignant peripheral nerve sheath tumors by
688 disrupting hyaluronan-CD44 interactions with small hyaluronan oligosaccharides.
689 Cancer Res 2009; 69: 4992–8.

690 36. Tamura R, Yokoyama Y, Yoshida H, Imaizumi T, Mizunuma H. 4-
691 Methylumbelliferone inhibits ovarian cancer growth by suppressing thymidine
692 phosphorylase expression. J Ovarian Res 2014; 7: 94.

693 37. Saito T, Dai T, Asano R. The hyaluronan synthesis inhibitor 4-methylumbelliferone
694 exhibits antitumor effects against mesenchymal-like canine mammary tumor cells.
695 Oncol Lett 2013; 5: 1068–74

696 38. Edward M, Quinn JA, Pasonen-Seppänen SM, McCann BA, Tammi RH. 4-
697 Methylumbelliferone inhibits tumour cell growth and the activation of stromal
698 hyaluronan synthesis by melanoma cell-derived factors. Br J Dermatol 2010; 162:
699 1224–32.

700 39. Morohashi H, Yoshihara S, Nakai M, Yamazaki M, Kakizaki I, Kon A, Sasaki M,
701 Takagaki K. Inhibitory effect of 4-methylesculetin on hyaluronan synthesis slows the
702 development of human pancreatic cancer in vitro and in nude mice. Int J Cancer 2007;
703 120: 2704–9

704 40. Kosaki R, Watanabe K, Yamaguchi Y. Overproduction of hyaluronan by expression
705 of the hyaluronan synthase Has2 enhances anchorage-independent growth and
706 tumorigenicity. Cancer Res 1999; 59: 1141–5

707 41. Wojtkowiak JW, Fouad F, Lalonde DT, Kleinman MD, Gibbs RA, Reiners JJ, Borch
708 RF, Mattingly RR. Induction of Apoptosis in Neurofibromatosis Type 1 Malignant
709 Peripheral Nerve Sheath Tumor Cell Lines by a Combination of Novel Farnesyl
710 Transferase Inhibitors and Lovastatin. J Pharmacol Exp Ther 2008; 326: 1–11

711 42. Endo M, Yamamoto H, Setsu N, Kohashi K, Takahashi Y, Ishii T, Iida K, Matsumoto
712 Y, Hakozaki M, Aoki M, Iwasaki H, Dobashi Y, Nishiyama K, Iwamoto Y. Prognostic
713 significance of AKT/mTOR and MAPK pathways and antitumor effect of mTOR
714 inhibitor in NF1-related and sporadic malignant peripheral nerve sheath tumors. Clin
715 Cancer Res 2013; 19: 450–61

716 43. Bhola P, Banerjee S, Mukherjee J, Balasubramanium A, Arun V, Karim Z, Burrell K,

717 Croul S, Gutmann DH, Guha H. Preclinical in vivo evaluation of rapamycin in human
718 malignant peripheral nerve sheath explant xenograft. Int J Cancer 2010; 126: 563–71

719 44. Mahller YY, Vaikunth SS, Currier MA, Miller SJ, Ripberger MC, Hsu YH, Mehrian-
720 Shai R, Collins MH, Crombleholme TM, Ratner N, Cripe TP. Oncolytic HSV and
721 erlotinib inhibit tumor growth and angiogenesis in a novel malignant peripheral nerve
722 sheath tumor xenograft model. Mol Ther 2007; 15: 279–86

723 45. Ohishi J, Aoki M, Nabeshima K, Suzumiya J, Takeuchi T, Ogose A, Hakozaki M,
724 Yamashita Y, Iwasaki H. Imatinib mesylate inhibits cell growth of malignant
725 peripheral nerve sheath tumors in vitro and in vivo through suppression of PDGFR-ß.
726 BMC Cancer 2013; 13: 224

727 46. Ambrosini G, Cheema HS, Seelman S, Teed A, Sambol EB, Singer S, Schwartz GK.
728 Sorafenib inhibits growth and mitogen-activated protein kinase signaling in malignant
729 peripheral nerve sheath cells. Mol Cancer Ther 2008; 7: 890–6

730 47. Widemann BC, Salzer WL, Arceci RJ, Blaney SM, Fox E, End D, Gillespie A,
731 Whitcomb P, Palumbo JS, Pitney A, Jayaprakash N, Zannikos P, Balis FM. Phase I trial
732 and pharmacokinetic study of the farnesyltransferase inhibitor tipifarnib in children
733 with refractory solid tumors or neurofibromatosis type I and plexiform neurofibromas.
734 J Clin Oncol 2006; 24: 507–16.

735 48. Weiss B, Widemann BC, Wolters P, Dombi E, Vinks A, Cantor A, Perentesis J,
736 Schorry E, Ullrich N, Gutmann DH, Tonsgard J, Viskochil D, Korf B, Packer RJ, Fisher
737 MJ. Sirolimus for progressive neurofibromatosis type 1-associated plexiform
738 neurofibromas: a Neurofibromatosis Clinical Trials Consortium phase II study. Neuro
739 Oncol 2014; 17: 596–603

740 49. Albritton KH, Rankin C, Coffin CM, Ratner N, Budd GT, Schuetze SM, Randall RL,

741 Declue JE, Borden EC. Phase II study of erlotinib in metastatic or unresectable
742 malignant peripheral nerve sheath tumors (MPNST). J Clin Oncol 2006; 24 (suppl;
743 abstr 9518)

744 50. Maki RG, D'Adamo DR, Keohan ML, Saulle M, Schuetze SM, Undevia SD,
745 Livingston MB, Cooney MM, Hensley ML, Mita MM, Takimoto CH, Kraft AS, Elias AD,
746 Brockstein B, Blachère NE, Edgar MA, Schwartz LH, Qin LiX, Antonescu CR,
747 Schwartz GK. Phase II study of sorafenib in patients with metastatic or recurrent
748 sarcomas. J Clin Oncol 2009; 27: 3133–40.

749 51. Chugh R, Wathen JK, Maki RG, Benjamin RS, Patel SR, Myers PA, Priebat DA,
750 Reinke DK, Thomas DG, Keohan ML, Samuels BL, Baker LH. Phase II multicenter
751 trial of imatinib in 10 histologic subtypes of sarcoma using a bayesian hierarchical
752 statistical model. J Clin Oncol 2009; 27: 3148–53.

753

754

755 **Figure legends**

756

757 Fig. 1

758 Effects of MU (1.0 mM) on intracellular and pericellular HA accumulation in sNF96.2
759 and sNF02.2 cells. (a) Histochemical staining with b-HABP in each cell treated with or
760 without MU (0.1% DMSO) for 24 h. The cells incubated without b-HABP were used as
761 negative controls. MU treatment caused a loss of filopodia-like structures in both
762 sNF96.2 and sNF02.2 cells (arrowheads) (original magnification × 400). (b) Visualized
763 pericellular matrices following treatment for 48 h with (1.0 mM) or without MU (0.1%
764 DMSO). Green cells depicted the stained cells with Calcein AM (ii, iv, vi, and viii). All
765 cells were presented at the same magnification (original magnification × 200). Both

766 sNF96.2 (i and ii) and sNF02.2 cells (v and vi) treated with the control medium showed
767 abundant pericellular matrices (arrows). In contrast, sNF96.2 (iii and iv) and sNF02.2
768 cells (vii and viii) treated with 1.0 mM of MU had markedly reduced pericellular
769 matrices. (original magnification × 400). (c) Morphometric analyses of pericellular
770 matrices. The proportions of the area delineated by the pericellular matrix area to the
771 area delineated by the plasma membrane area were plotted. Data represent the means
772 ± SD from 10 cells under each condition. (** $P < 0.01$ compared with the control treated
773 without MU, as measured using student's t test).
774
775 Fig. 2
776 Effects of MU (1.0 mM) on the concentration (ng/10^5 cells) of HA in sNF96.2 and
777 sNF02.2 cells at 12- and 24-h time points of incubation in the presence or absence of
778 MU. (a) The concentration (ng/10^5 cells) of pericellular HA in sNF96.2 cells. (b) The
779 concentration (ng/10^5 cells) of intracellular HA in sNF96.2 cells. (c) The concentration
780 (μg/10^5 cells) of HA in medium in sNF96.2 cells. (d) The concentration (ng/10^5 cells) of
781 pericellular HA in sNF02.2 cells. (e) The concentration (ng/10^5 cells) of intracellular HA
782 in sNF02.2 cells. (f) The concentration (μg/10^5 cells) of HA in medium in sNF02.2 cells.
783 Each experiment was performed in triplicate, and bars indicate the means ± SD. (* $P <$
784 0.05 and ** $P < 0.01$ compared with the control treated without MU, as measured using
785 Bonferroni-Dunn post hoc test).
786
787 Fig. 3
788 Effects of MU (0.1 mM and 1.0 mM) on cell proliferation, migration, invasion, apoptotic
789 activity, and HAS mRNA expression of sNF96.2 and sNF02.2 cells. (a and b) Cell
790 proliferation of sNF96.2 and sNF02.2 cells at 24-, 48-, and 72-h time points of
791 treatment with or without MU, respectively. (c) Migratory activity of sNF96.2 and

792 sNF02.2 cells after treatment for 24 h with or without MU. (d) Invasiveness of sNF96.2
793 and sNF02.2 cells after treatment for 24 h with or without MU. The exogenous HA
794 (600–1,200 kDa, 200 μg/ml) was added concurrently with MU in (a and b) cell
795 proliferation, (c) migration, and (d) invasion assays. (e) Apoptotic activity of sNF96.2
796 and sNF02.2 cells determined by flow cytometric analysis of Annexin V after treatment
797 for 48 h with or without MU. (f and g) The relative values of HAS2 and HAS3 mRNA
798 expression in sNF96.2 and sNF02.2 cells after treatment for 12 h with or without MU.
799 The data presented were standardized by GAPDH mRNA expression. Each experiment
800 was performed in triplicate, and bars indicate the means ± SD (*$P < 0.05$ and **$P <$
801 0.01 compared with the control treated without MU, using Bonferroni-Dunn post hoc
802 test).
803
804 Fig. 4
805 Effects of MU on tumor growth in xenograft mice model of sNF96.2. After the
806 establishment of the sNF96.2 tumor, administration of daily MU (10mg/body weight)
807 for six weeks significantly suppressed tumor growth in volume (a) and weight (b) (*$P <$
808 0.05 and **$P < 0.01$, respectively compared with the control treated without MU, using
809 Mann-Whitney U test or student-t test). (n = 8 each). (c) Representative pictures of
810 resected tumors from the mice treated with or without MU for six weeks are shown. (d)
811 Histological findings of the xenograft tumors after treatment for six weeks with (ii and
812 iv) or without (i and iii) MU. Sections were stained with HABP (i and ii; original
813 magnification × 100, bars indicate 500 μm). Representative images with higher
814 magnification were shown as insets (iii and iv; original magnification × 400, bars
815 indicate 100 μm). Representative images with higher magnification was shown as inset
816 Sections with or without MU (vi and v, respectively) were immunolabeled for Ki67
817 (original magnification × 400, bars indicate 100 μm). (e) Percentage of Ki67-positive

818 cells in tumor sections from the control and MU-treated mice. Percentage of positive
819 cells were calculated by dividing the number of Ki67-positive cells by the total number
820 of cells in each field. (**P < 0.01, control vs MU treated tumors, using student's t test).
821 (n = 3 each). (g) Body weight of the mice treated and untreated with MU during
822 administration of daily MU for six weeks (difference was not significant, control vs MU
823 treated mice, using student's t test). (n = 8 each).
824

825 Supplementary figure legends

826 Fig. S1

827 (a) Representative histograms of flow cytometric analysis with Annexin V
828 depicting apoptosis distribution in sNF96.2 and sNF02.2 cells after treatment for 48 h
829 with or without MU. Histograms of sNF96.2 cells treated with (i) DMSO, (ii) 0.1 mM
830 MU, and (iii) 1.0 mM MU were shown. Histograms of sNF02.2 cells treated with (iv)
831 DMSO, (v) 0.1 mM MU, and (vi) 1.0 mM MU were shown. Presented data were
832 representatives of at least three independent experiments. (b) Effects of MU on
833 apoptotic activity in sNF96.2 and sNF02.2 cells, and bars represent mean ±SD. (*P <
834 0.05 and **P < 0.01 compared with the control treated with DMSO, as measured using
835 Bonferroni-Dunn post hoc test).

836

837 Fig. S2

838 (e) The relative values of HAS2, HAS3, and CD44 mRNA expression in sNF96.2
839 and sNF02.2 cells after treatment for 6, 12, 24 h with or without MU. The data
840 presented were standardized by GAPDH mRNA expression. Each experiment was
841 performed in triplicate, and bars indicate the means ± SD (*P < 0.05 and **P < 0.01

842 compared with the control treated without MU, using Bonferroni-Dunn post hoc test).

843

844 Fig. S3

845 (f) Cell migration and invasiveness of sNF96.2 and sNF02.2 cells after
846 knockdown of CD44. The data are presented as the means ± SD (**$P < 0.01$ compared
847 with the control treated with DMSO, using Bonferroni-Dunn post hoc test).

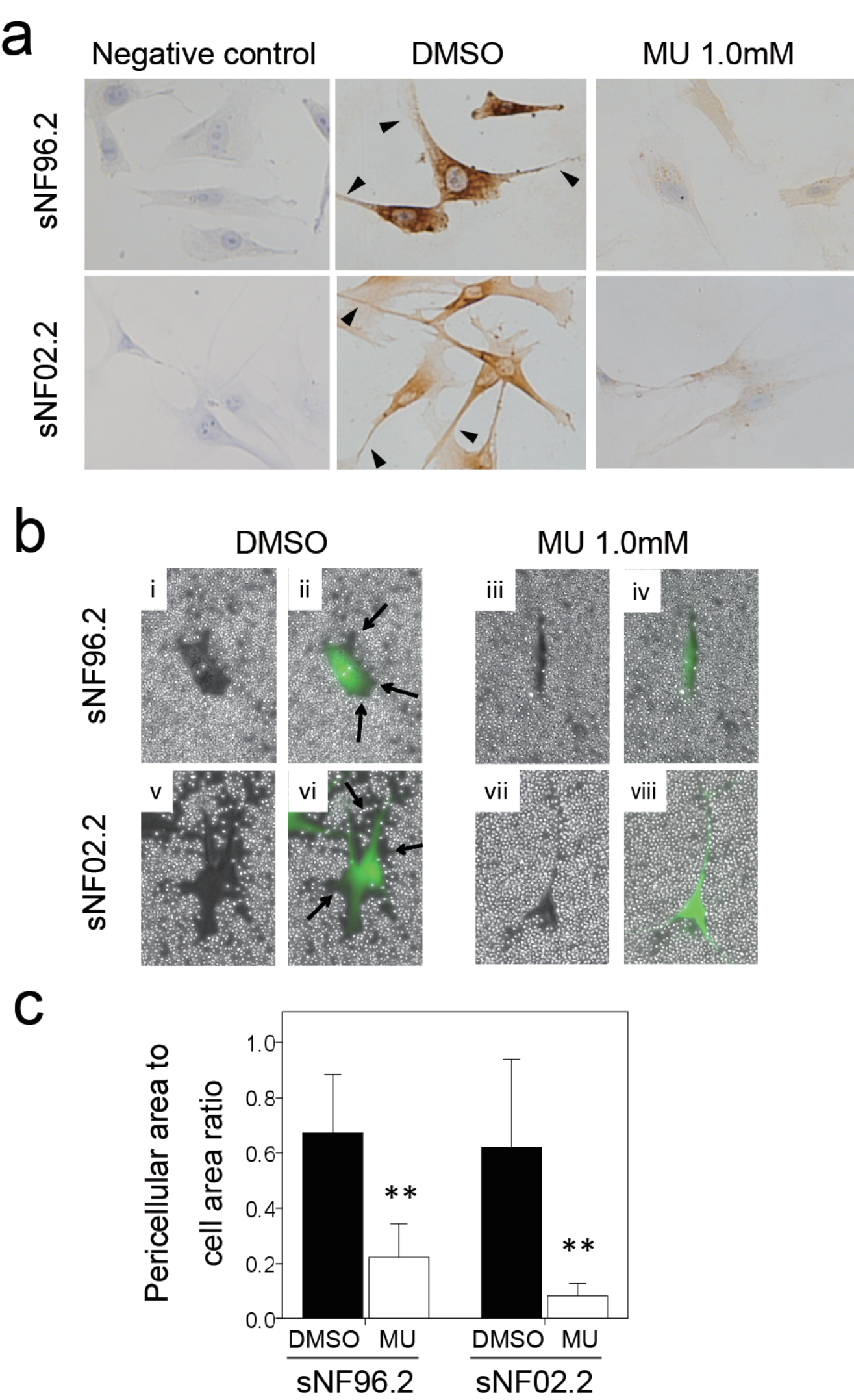
a
Negative control
DMSO
MU 1.0mM
sNF96.2
sNF02.2
b
DMSO
MU 1.0mM
sNF96.2
sNF02.2
i
ii
iii
iv
v
vi
vii
viii
c
Pericellular area to cell area ratio
1.0
0.8
0.6
0.4
0.2
0.0
**
**
DMSO
MU
DMSO
MU
sNF96.2
sNF02.2

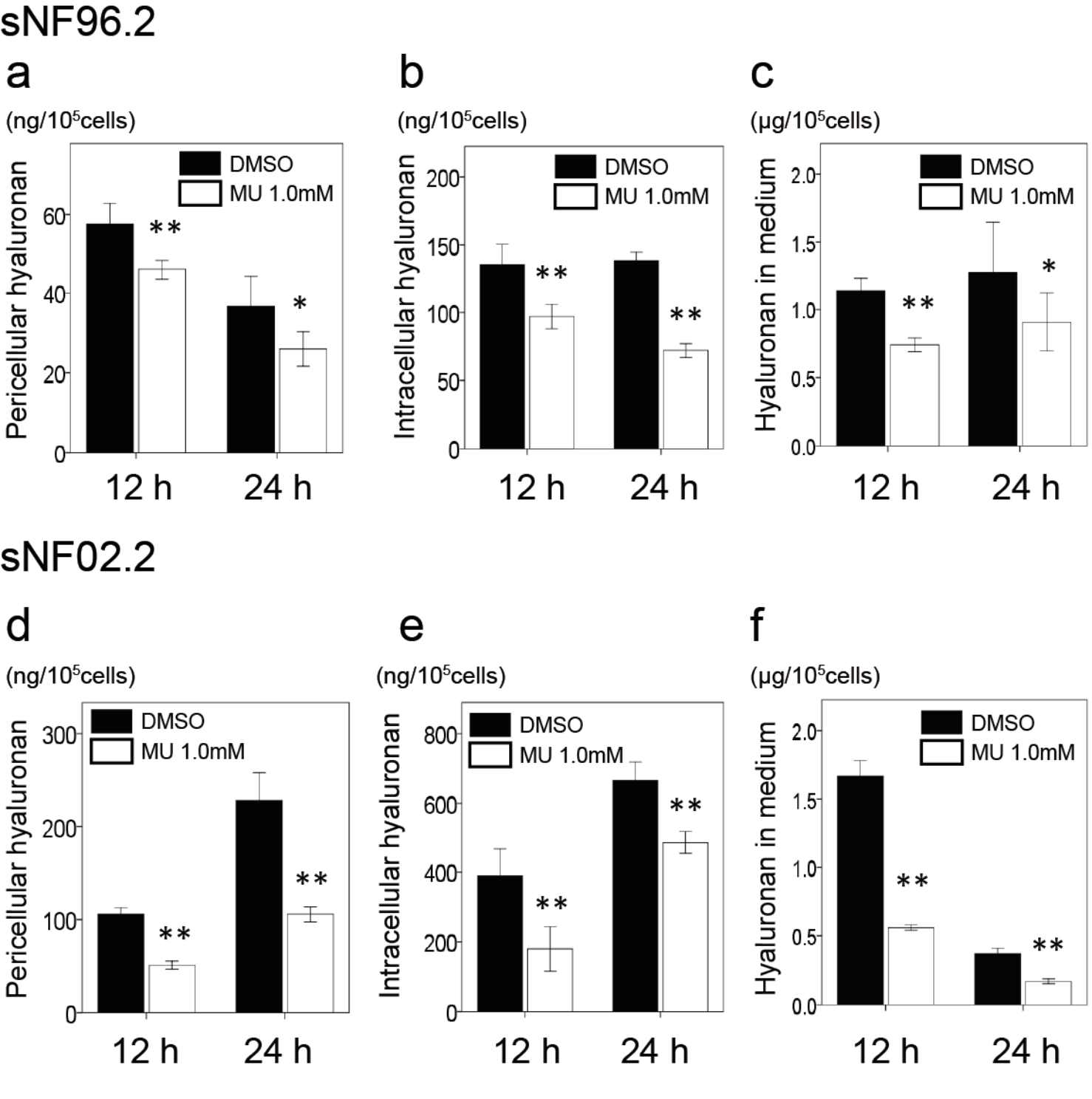
sNF96.2
a
(ng/10⁵cells)
Pericellular hyaluronan
DMSO
MU 1.0mM
0
20
40
60
**
*
12 h
24 h
b
(ng/10⁵cells)
Intracellular hyaluronan
DMSO
MU 1.0mM
0
50
100
150
200
**
**
12 h
24 h
c
(μg/10⁵cells)
Hyaluronan in medium
DMSO
MU 1.0mM
0.0
0.5
1.0
1.5
2.0
**
*
12 h
24 h
sNF02.2
d
(ng/10⁵cells)
Pericellular hyaluronan
DMSO
MU 1.0mM
0
100
200
300
**
**
12 h
24 h
e
(ng/10⁵cells)
Intracellular hyaluronan
DMSO
MU 1.0mM
0
200
400
600
800
**
**
12 h
24 h
f
(μg/10⁵cells)
Hyaluronan in medium
DMSO
MU 1.0mM
0.0
0.5
1.0
1.5
2.0
**
**
12 h
24 h

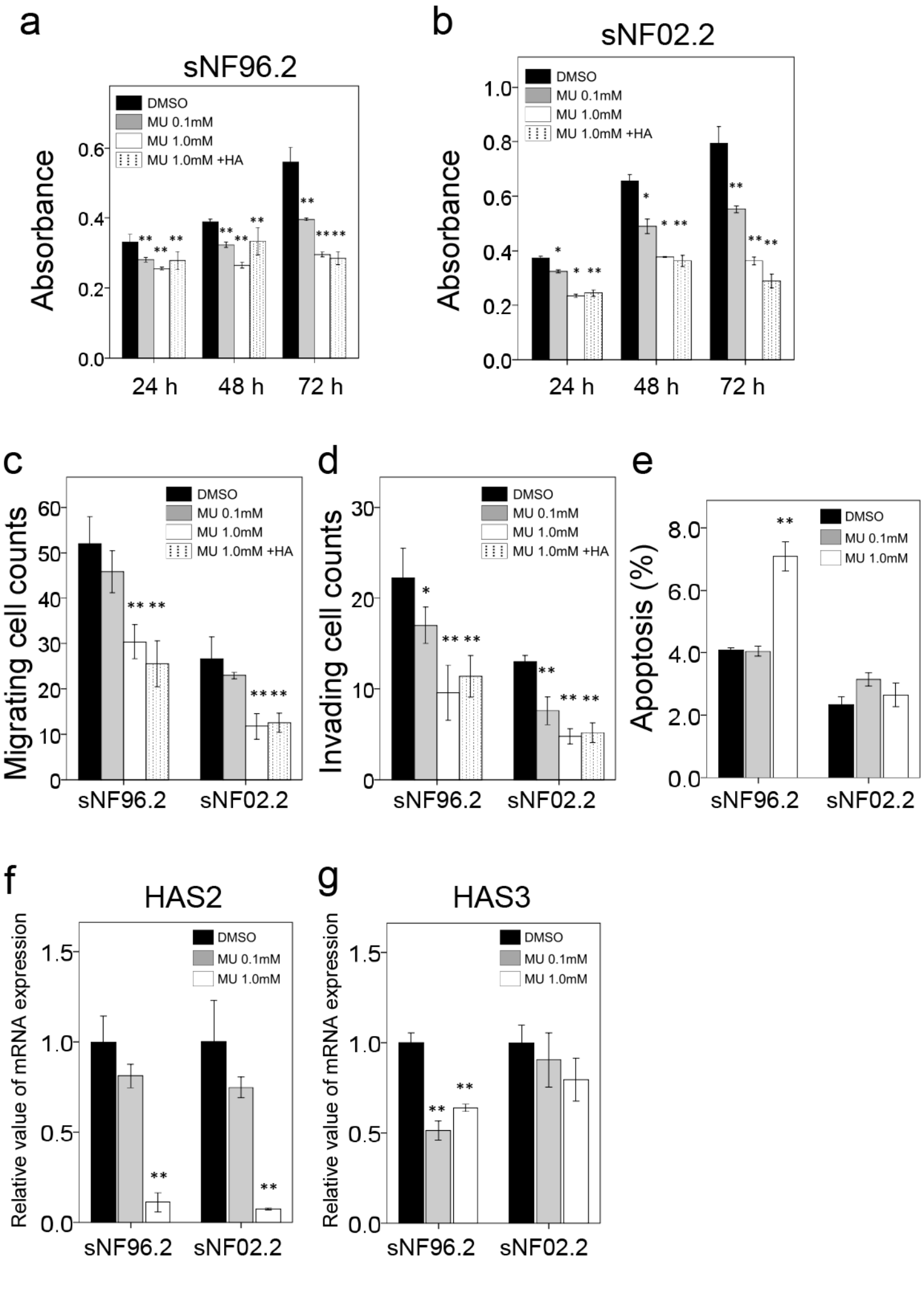
a
sNF96.2
DMSO
MU 0.1mM
MU 1.0mM
MU 1.0mM +HA
Absorbance
0.0
0.2
0.4
0.6
24 h
48 h
72 h
b
sNF02.2
DMSO
MU 0.1mM
MU 1.0mM
MU 1.0mM +HA
Absorbance
0.0
0.2
0.4
0.6
0.8
1.0
24 h
48 h
72 h
c
DMSO
MU 0.1mM
MU 1.0mM
MU 1.0mM +HA
Migrating cell counts
0
10
20
30
40
50
60
sNF96.2
sNF02.2
d
DMSO
MU 0.1mM
MU 1.0mM
MU 1.0mM +HA
Invading cell counts
0
10
20
30
sNF96.2
sNF02.2
e
DMSO
MU 0.1mM
MU 1.0mM
Apoptosis (%)
0.0
2.0
4.0
6.0
8.0
sNF96.2
sNF02.2
f
HAS2
DMSO
MU 0.1mM
MU 1.0mM
Relative value of mRNA expression
0.0
0.5
1.0
1.5
sNF96.2
sNF02.2
g
HAS3
DMSO
MU 0.1mM
MU 1.0mM
Relative value of mRNA expression
0.0
0.5
1.0
1.5
sNF96.2
sNF02.2

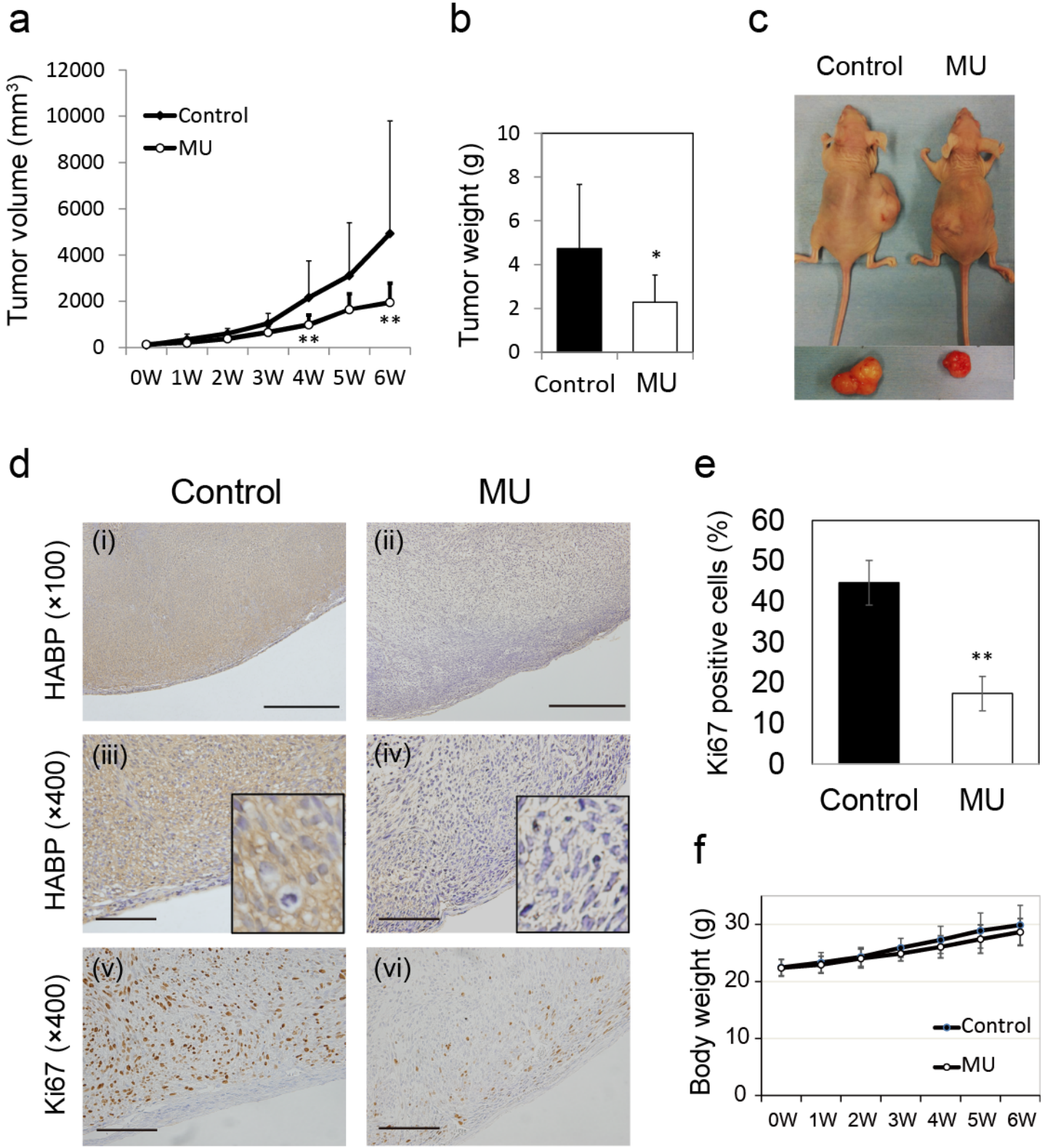
a
Tumor volume (mm3)
12000
10000
8000
6000
4000
2000
0
Control
MU
**
**
0W 1W 2W 3W 4W 5W 6W
b
Tumor weight (g)
10
8
6
4
2
0
*
Control MU
c
Control MU
d
Control
MU
HABP (×100)
(i)
(ii)
HABP (×400)
(iii)
(iv)
Ki67 (×400)
(v)
(vi)
e
Ki67 positive cells (%)
60
50
40
30
20
10
0
**
Control MU
f
Body weight (g)
30
20
10
0
Control
MU
0W 1W 2W 3W 4W 5W 6W

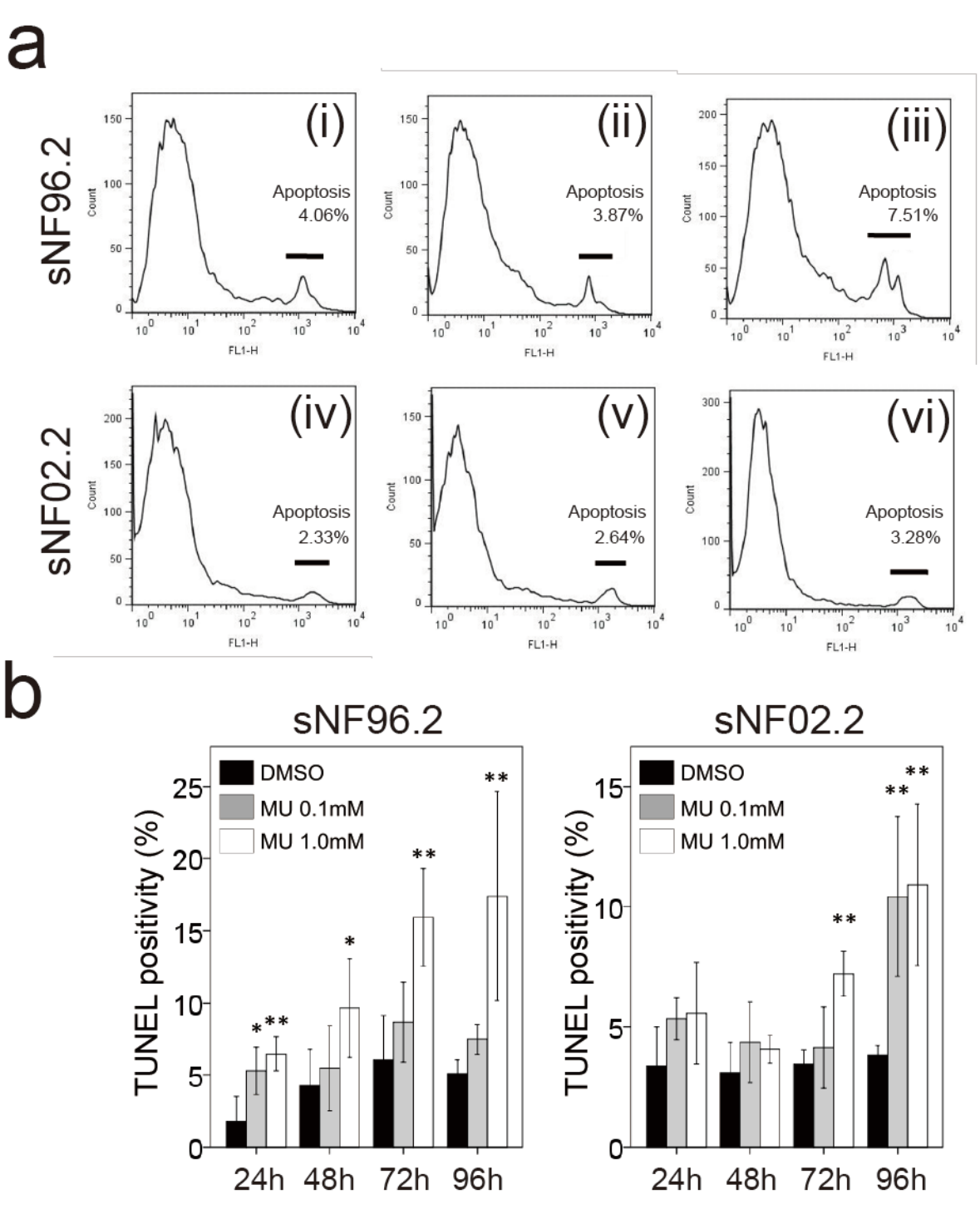
a
sNF96.2
sNF02.2
(i)
Apoptosis
4.06%
(ii)
Apoptosis
3.87%
(iii)
Apoptosis
7.51%
(iv)
Apoptosis
2.33%
(v)
Apoptosis
2.64%
(vi)
Apoptosis
3.28%
Count
FL1-H
b
sNF96.2
sNF02.2
DMSO
MU 0.1mM
MU 1.0mM
TUNEL positivity (%)
24h
48h
72h
96h

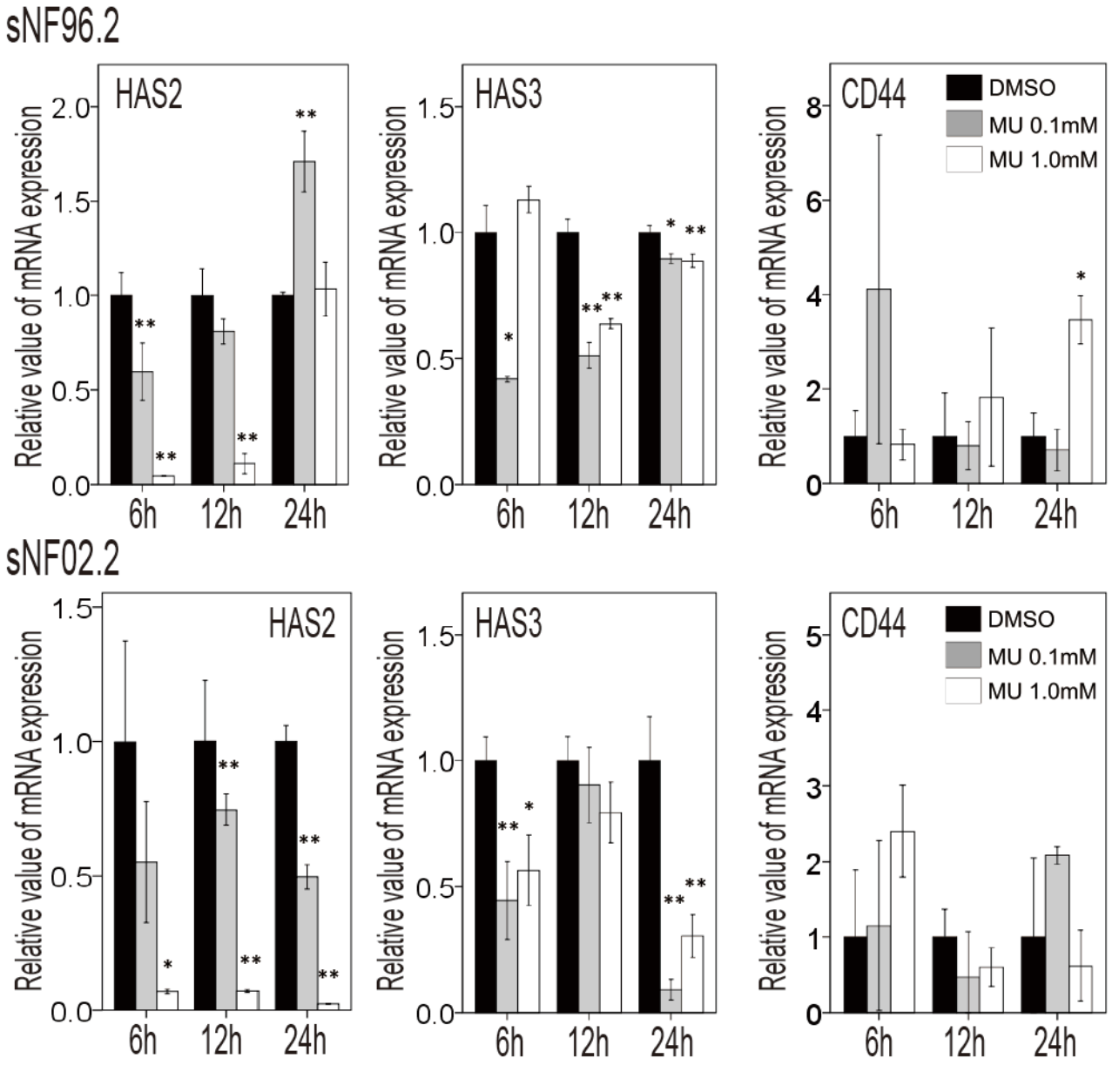
sNF96.2
HAS2
HAS3
CD44
DMSO
MU 0.1mM
MU 1.0mM
Relative value of mRNA expression
6h
12h
24h
sNF02.2
HAS2
HAS3
CD44
DMSO
MU 0.1mM
MU 1.0mM
Relative value of mRNA expression
6h
12h
24h

sNF96.2

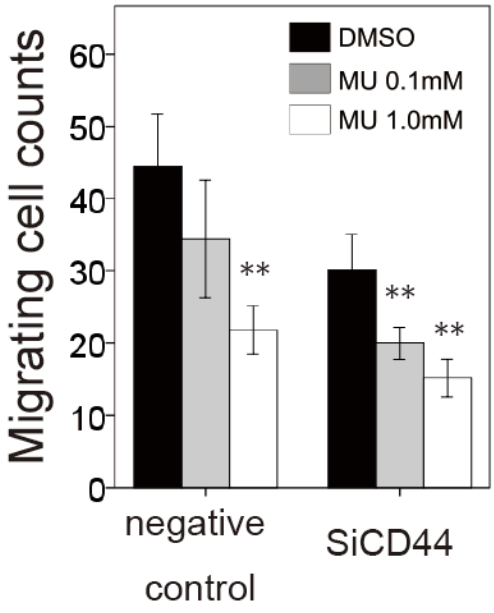

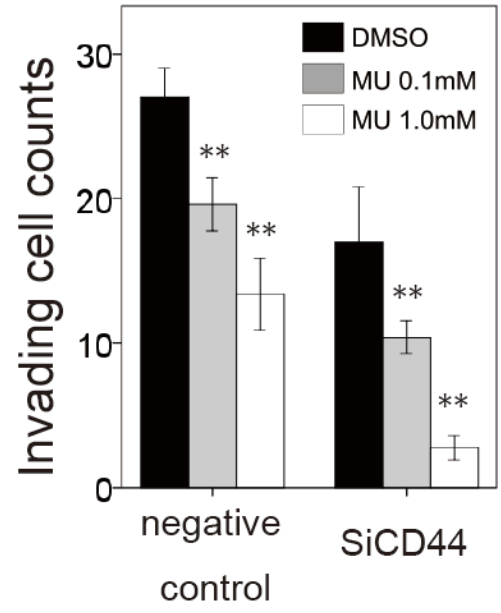

sNF02.2